

Three-jet cross sections in hadron-hadron collisions at next-to-leading order

Zoltan Nagy

Department of Physics, University of Durham DH1 3LE, England

(Dated: February 8, 2020)

We present a new QCD event generator for hadron collider which can calculate one-, two- and three-jet cross sections at next-to-leading order accuracy. In this letter we study the transverse energy spectrum of three-jet hadronic events using the k_t algorithm. We show that the next-to-leading order correction significantly reduces the renormalization and factorization scale dependence of the three-jet cross section.

PACS numbers: 13.87.Ce, 12.38.Bx

Keywords: Perturbative QCD, Jet calculation, NLO

The latest version of the experiment at Tevatron and the future collider LHC will provide precise data so that not only inclusive measurements can be used to study the physics of hadronic final state. The studies of the event shapes and multi-jet event can be important projects.

One of the important theoretical tools in the analysis of hadronic final states is perturbative Quantum Chromodynamics (QCD). In order to make quantitative predictions in perturbative QCD, it is essential to perform the computations (at least) at the next-to-leading order (NLO) accuracy. In hadron collision the most easily calculated one- and two-jet cross sections have so far been calculated at NLO level [1, 2]. At next-to-leading level some three-jet observables were calculated by Giele and Kilgore [3, 4] and by Trocsanyi [5]. In this letter we present a new NLO event generator for calculating jet observables in hadron-hadron collision. We compute the three-jet cross sections using the k_t algorithm [6] to resolve jets in the final state. With our Monte Carlo program one can compute the NLO cross section for any other infrared safe one-, two- and three-jet observables. The presented distributions are given simply as illustration.

In the case of one-jet inclusive cross section in high p_T region the forthcoming experimental data requires the knowledge of the higher order corrections. Recently, progress has been made in calculating the two loop $2! 2$ matrix elements [7, 8, 9]. These matrix element are need to set up a Monte Carlo program for calculating the next-to-next-to-leading order (NNLO) one- and two-jet cross section. However, the three-jet NLO calculation, comprising the one-loop $2! 3$ and tree-level $2! 3$ processes is a necessary first step of this project. A numerically stable and fast three-jet NLO program can provide enough hope that it might be possible to develop a numerically stable Monte Carlo program for calculating one- and two-jet cross sections at NNLO level.

In the last few years the theoretical developments make possible the next-to-leading order calculation for the three-jet quantities. There are several general methods available for the cancellation of the infrared divergences that can be used for setting up a Monte Carlo

program [10, 11, 12]. In computing the NLO correction we use the dipole formalism of Catani-Seymour [12] that we modified slightly in order to have a better control on the numerical calculation. The main idea is to cut the phase space of the dipole subtraction terms as introduced in Ref. [13], the details of how to this to apply for the case of hadron-hadron scattering will be given elsewhere.

The advantages of using the dipole method are the following: i) no approximation is made; ii) the exact phase space factorization allows full control over the efficient generation of the phase space; iii) neither the use of color ordered subamplitudes, nor symmetrization, nor partial fractioning of the matrix elements is required; iv) Lorentz invariance is maintained, therefore, the switch between various frames can be achieved by simply transforming the momenta; v) the use of crossing functions is avoided; vi) it can be implemented in an actual program in a fully process independent way.

In this calculation we used the crossing symmetric tree- and one-loop level amplitudes. The parton subprocess $0! \ggggg$ [14], $0! \qgggg$ [15], $0! \qqQ Q g$ [16] and the subprocesses related to these have been computed to one-loop and $0! \gggggg$, $0! \qggggg$, $0! \qqQ Q gg$ [17] and the crossed processes have been computed at tree level.

We have checked numerically that in all soft and collinear regions the difference of the real and subtraction terms contain only integrable square-root singularities. Furthermore, we have also checked that our results are independent of the parameter that controls the volume of the cut dipole phase space, which ensures that indeed the same quantity has been subtracted from the real correction as added to the virtual one.

Finally, to have a further check of the computation, Our method of implementing the dipole subtraction terms allows for the construction of a process independent program using of QCD jet cross sections at the NLO accuracy. We use the same program structure, with trivial modifications, to compute one-, two- and three-jet cross sections.

In order to check the base structure of the program we compare the our inclusive one-jet NLO result to predic-

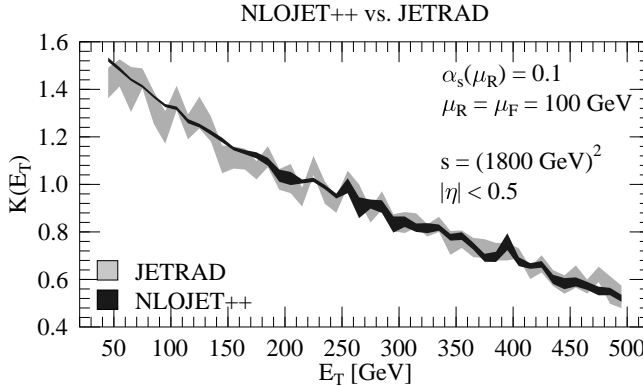


FIG. 1: Comparison of the K factors of the one-jet inclusive cross section defined using the k_\perp and MRS D⁰ parton densities obtained with Monte Carlo programs JETRAD and NLO JET++ (this work). The bands indicate the statistical error of the calculations.

tion of the program JETRAD [1]. In this comparison we compare the one-jet inclusive cross section using the k_\perp jet algorithm and MRS D⁰ parton distribution function [18]. We find good agreement between the two programs. The differences are within the statistical error as Fig. 1 shows.

Historically, only the cone algorithm has been used to reconstruct the jet at hadron collider. In the three or higher jet calculation at NLO level the cone algorithm is not suitable because it has a lot of difficulties: an arbitrary procedure must be implemented to split and merge the overlapping cones, and an ad-hoc parameter R_{sep} is required to accommodate the difference between the jet definitions at parton and detector level. To avoid this uncertainty we use the k_\perp algorithm which has been developed by several groups [19]. Our implementation is based on the Ref. [6]. The algorithm starts with a list of the particles and the empty list of the jets.

1. For each particle (pseudo-particle) i in the list, define

$$d_i = p_{T,i}^2 : \quad (1)$$

For each pair (i, j) of momenta $(i \neq j)$, define

$$d_{ij} = \min(p_{T,i}^2; p_{T,j}^2) \frac{R_{ij}^2}{D^2} ; \quad (2)$$

where $R_{ij}^2 = (i_j)^2 + (i_j)^2$ is square of the angular separation which is expressed in the term of the pseudo-rapidity η and the azimuthal angle ϕ . D is a free parameter. The usual choice of this parameter is $D = 1$.

2. Find the minimum of all the d_i and d_{ij} and label it d_{min} .
3. If d_{min} is d_{ij} , remove particles (pseudo-particles) i and j from the list and replace them with a new,

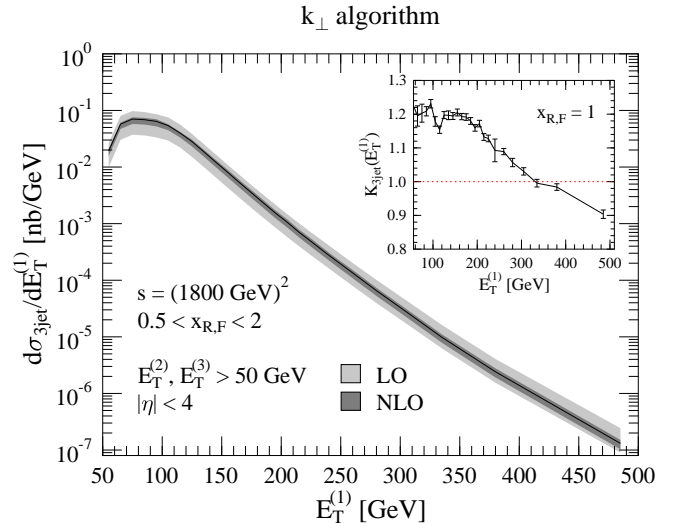


FIG. 2: The perturbative prediction for the three-jet differential cross section in the term of the transverse energy of the leading jet at Born level (light gray band) and next-to-leading order (dark gray band). The bands indicate the theoretical uncertainty due to the variation of the renormalization and factorization scales $x_{R,F}$ between 0.5 and 2. The solid line is the NLO result for the $x_R = x_F = 1$ choice of the scales.

merged pseudo-particle $p_{(ij)}$ given by the recombination scheme. In this paper we use the E recombination scheme which is define the new pseudo-particle as the sum of the two particle

$$p_{(ij)} = p_i + p_j : \quad (3)$$

4. If d_{min} is d_i , remove particle (pseudo-particle) i from the list of particle and add it to list of jets.
5. If any particles remain, go to step 1.

The algorithm produces a list of jets, each separated by $R_{ij} > D$.

Once the phase space integrations are carried out, we write the NLO jet cross section in the following form :

$$\begin{aligned} \frac{d\sigma}{dE_T} &= \sum_{A,B} \sum_{a,b} d_{a,b} f_{a=A} \left(\frac{p_a^2}{Q_F^2} \right) f_{b=B} \left(\frac{p_b^2}{Q_F^2} \right) \\ &\quad \times \frac{p_a \cdot p_b}{s} ; \quad s = \frac{Q_H^2}{Q_F^2} ; \quad \frac{Q_H^2}{Q_F^2} = \frac{Q_H^2}{Q_H^2} ; \quad \frac{Q_H^2}{Q_F^2} = \frac{Q_H^2}{Q_H^2} ; \quad (4) \end{aligned}$$

where $f_{i=H} \left(\frac{p_i^2}{Q_F^2} \right)$ represents the parton distribution function of the incoming hadron defined at the factorization scale $F = x_F Q_H$, a,b is the fraction of the proton momentum carried by the scattered partons $p_{a,b}$, Q_H is the hard scale that characterizes the parton scattering which could be E_T of the jet, jet mass of the event, etc and $R = x_R Q_H$ is the renormalization scale.

Eq. (4) shows that using the dipole method one may either compute the full cross section at NLO accuracy including the convolution with the parton distribution

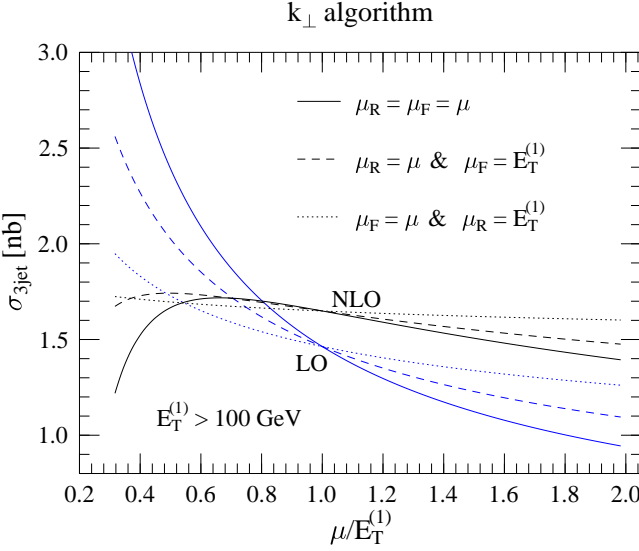


FIG. 3: The dependence of the three-jet cross section $\sigma_{3\text{jet}}$ on the renormalization and factorization scales.

functions, or simply the parton level cross section $\hat{\sigma}_{ab}$ which can then be convoluted with the parton densities after the Monte Carlo integration. The latter procedure is the proper one if we are interested in measurement of the parton distribution functions (to avoid the recalculation of the Monte Carlo integrals after each step of the fitting iteration).

The three-jet cross sections presented here were calculated for TEVATRON collider in proton-antiproton collision at the center of mass energy $s = 1800 \text{ GeV}$. We restrict the pseudo-rapidity range and the minimum transverse energy of the jets in laboratory frame to be

$$4 < \eta_{\text{jet}} < 4; \quad E_T > 50 \text{ GeV} : \quad (5)$$

We choose the transverse energy of the leading jets

$$Q_H = E_T^{(1)}; \quad (6)$$

as the hard scattering scale.

In Fig. 2, we plotted differential cross section in the term of the transverse energy of leading jet convoluted with the CTEQ 5M 1 parton distribution functions [20] and using the two-loop formula for the strong coupling,

$$s(\mu) = \frac{s(M_Z)}{w(\mu)} \quad 1 - \frac{s(M_Z)}{2} \frac{1}{w_0} \frac{\ln(w(\mu))}{w(\mu)}; \quad (7)$$

$$w(\mu) = 1 - \frac{s(M_Z)}{2} \ln \frac{M_Z}{w_0}; \quad (8)$$

where $s(M_Z) = 0.118$ and $w_0 = (11C_A - 4T_R N_f)/3 = 1 = (17C_A^2 - 6C_F T_R N_f - 10C_A T_R N_f)/3$, with $N_f = 5$ flavors. For the leading order results we used the CTEQ 5L distributions and the one-loop $s(\mu) =$

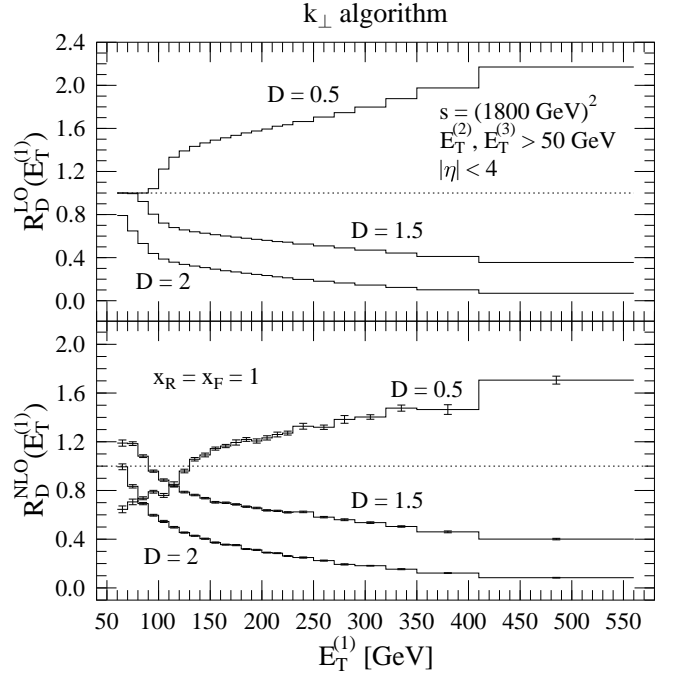


FIG. 4: The dependence of the three-jet differential cross section on the parameter D . The R_D means the ratio of the differential cross sections for a given D and for $D = 1$. Upper figure shows the Born level result and the lower figure shows the NLO prediction. The error bars indicate the statistical error of the Monte Carlo calculation.

0.127 and $w_0 = 0$ in Eq. (7)). In this figure the theoretical uncertainty of the three-jet cross section is shown. Over the wide range of the value the renormalization and factorization scale ($0.5 < x_R, x_F < 2$) this uncertainty is in the next-to-leading order result is much than in the Born level calculation.

In Fig. 3 we study the scale dependences of the three-jet cross section. The strong dependence on the renormalization scale observed at LO is significantly reduced. The factorization scale dependence is not significant at NLO and does not change much. Setting the two scales equal, $\mu_R = \mu_F = \mu$, we can observe a wide plateau peaking around $x_R = x_F = 0.7$.

The inset figure in Fig. 2 shows the K factor (ratio of the three-jet cross section at NLO to that at LO accuracy), indicating the relative size of the correction. We can see the size of the NLO correction is between 10 and 25% for smaller values of the transverse energy and at the end of the spectra the size of the correction is almost zero. The error bars indicate the statistical error of the Monte Carlo calculation. Because of the strong logarithmic behavior of the cross section the Monte Carlo calculation is very sensitive to the "missed binning" (when a huge positive comes from the real term and the corresponding huge negative weight from the subtraction term are filled in different histogram bins).

In Fig. 4 we study the dependence of the differential

cross section on parameter D . We plotted the ratios of the cross section

$$R_D(E_T^{(1)}) = \frac{d \frac{3\text{jet}}{pp}(E_T^{(1)}; D)}{dE_T^{(1)}} \cdot \frac{d \frac{3\text{jet}}{pp}(E_T^{(1)}; 1)}{dE_T^{(1)}} ; \quad (9)$$

for three different values of the parameter D ($D = 0.5; 1.5; 2$). The parameter D controls the angular separation in the jet algorithm procedure in Eq. 2. Changing this parameter we expect more resolved jets (more three-jet events) with high transverse energy and less recombination for smaller values of D and vice-versa. This behavior can be clearly observed from in Fig. 4.

In this letter we presented a NLO computation of the three-jet cross section defined with the k_T clustering algorithm in hadron-hadron collision. Our results were obtained using a partonic Monte Carlo program that is suitable for implementing any detector cuts. We found that the NLO the correction is under 30% in the case of differential cross section but the K factor is sensitive to the allowed kinematic region. We demonstrated that the NLO corrections reduce the scale dependence significantly. We also presented how the differential cross section depends on the angular separation parameter D used to define the jet. The same program can be used for computing the QCD radiative corrections to the (differential) cross section of any kind of one-, two-, or three-jet cross section or event-shape distribution in hadron-hadron collision. We compared the two-jet results obtained by our program to previous results and found agreement.

I thank Nigel Glover and Adrian Signer for the helpful discussions. This work was supported in part by the EU Fourth Framework Program me Research Training Network Particle Physics Phenomenology at High Energy Colliders', contract HPRN-CT-2000-00149.

Zoltan Nagy@durham.ac.uk; <http://www.cpt.dur.ac.uk/~nagy/nlo++.html>

- [1] W. T. Giele, E. W. N. Glover, and D. A. Kosower, Nucl. Phys. B 403, 633 (1993), hep-ph/9302225.
- [2] Z. Kunszt and D. E. Soper, Phys. Rev. D 46, 192 (1992).
- [3] W. B. Kilgore and W. T. Giele, hep-ph/9903361; hep-ph/0009176; hep-ph/0009193.
- [4] W. B. Kilgore and W. T. Giele, Phys. Rev. D 55, 7183 (1997), hep-ph/9610433.
- [5] Z. Trocsanyi, Phys. Rev. Lett. 77, 2182 (1996), hep-ph/9610499.
- [6] S. D. Ellis and D. E. Soper, Phys. Rev. D 48, 3160 (1993), hep-ph/9305266.
- [7] C. A. Anastasiou, E. W. N. G Glover, C. Oleari, and M. E. Tejeda-Yeomans, Nucl. Phys. B 601, 341 (2001), hep-ph/0011094.
- [8] C. A. Anastasiou, E. W. N. G Glover, C. Oleari, and M. E. Tejeda-Yeomans, Nucl. Phys. B 605, 486 (2001), hep-ph/0101304.
- [9] E. W. N. G Glover and M. E. Tejeda-Yeomans, JHEP 05, 010 (2001), hep-ph/0104178.
- [10] Z. Nagy and Z. Trocsanyi, Nucl. Phys. B 486, 189 (1997), hep-ph/9610498.
- [11] S. Frixione, Z. Kunszt, and S. A., Nucl. Phys. B 467, 399 (1996), hep-ph/9512328.
- [12] S. Catani and M. H. Seymour, Nucl. Phys. B 485, 291 (1997), [Erratum -ibid B 510, 503 (1997)], hep-ph/9605323.
- [13] Z. Nagy and Z. Trocsanyi, Phys. Rev. D 59, 014020 (1999), hep-ph/9806317.
- [14] Z. Bern, L. J. Dixon, and D. A. Kosower, Phys. Rev. Lett. 70, 2677 (1993), hep-ph/9302280.
- [15] Z. Bern, L. J. Dixon, and D. A. Kosower, Nucl. Phys. B 437, 259 (1995), hep-ph/9409393.
- [16] Z. Kunszt, A. Signer, and Z. Trocsanyi, Phys. Lett. B 336, 529 (1994), hep-ph/9405386.
- [17] J. G. M. Kuifje (1991), rX-1335 (LEIDEN) Ph.D. thesis.
- [18] A. D. M. Martin, W. J. Stirling, and R. G. Roberts, Phys. Rev. D 47, 867 (1993).
- [19] S. Catani, Y. L. Dokshitzer, M. H. Seymour, and B. R. Webber, Nucl. Phys. B 406, 187 (1993).
- [20] H. L. Lai et al. (CTEQ), Eur. Phys. J. C 12, 375 (2000), hep-ph/9903282.